www.project-foci.eu

Co-funded by
the European Union

UK Research
and Innovation

Horizon Europe

(HORIZON-CL5-2021-D1-01)

Non-CO2 Forcers and their Climate, Weather, Air Quality and Health Impacts

FOCI

Deliverable 6.3

Quantification of the past and future contribution of non-CO2 climate forcers to the (de)stabilization of tipping elements with the use of state-of-the-science climate-chemistry models

Grant agreement No 101056783

Grant Agreement No.	101056783	
Project acronym	FOCI	
Project full title	Non-CO2 Forcers and their Climate, Weather, Air Quality and Health Impacts	
Call	HORIZON-CL5-2021-D1-01	
Deliverable name	D6.3 Quantification of the past and future contribution of non-CO2 climate forcers to the (de)stabilization of tipping elements with the use of state-of-the-science climate-chemistry models	
WP contributing to the deliverable	WP6	
Task producing the deliverable	Task 6.3	
Type	X	Report
		Prototype
		Demonstrator
		Other: Data
Dissemination level	X	Public
		Sensitive
		UE/EU-Restricted
Due date of deliverable	Month 36	
Actual submission date	Month 36	
Lead beneficiary		
Author(s)	Alba Santos-Espeso (BSC), María Gonçalves (BSC), Pablo Ortega (BSC), Oriol Jorba (BSC)	
Other Contributor(s)		
Reviewer(s)	Twan van Noije (KNMI)	
Keywords	FOCI, deliverables	

ACKNOWLEDGEMENTS

This project has been co-funded by the European Union with funding from the European Union's Horizon Europe research and innovation programme under grant agreement No. 101056783 and from UKRI under the UK Government's Horizon Europe Guarantee (UKRI Reference Numbers: 10040465, 10053814 and 10050799).

Version	Date	Modified by	Comments
1.0	8 July 2025	Alba Santos-Espeso	First order draft written
2.0	27 August 2025	María Gonçalves (BSC)	Revisions made to incorporate reviewer's comments
3.0	28 August 2025	María Gonçalves (BSC)	Final version ready

	Name	Date
Verification Final Draft by WP leaders	Ranjeet Sokhi, Tomáš Halenka	28 Aug 2025
Check before upload by project Coordinator	Tomas Halenka	28 Aug 2025

TABLE OF CONTENTS

EXECUTIVE SUMMARY

This document is the deliverable "D6.3: Quantification of the past and future contribution of non-CO2 climate forcers to the (de)stabilization of tipping elements with the use of state-of-the-science climate-chemistry models" for the European Union project "FOCI: Non-CO2 Forcers and their Climate, Weather, Air Quality and Health Impacts" (hereinafter also referred to as FOCI, project reference: 101056783).

The report describes the multi-model analyses conducted to assess the impact of non-CO2 climate forcers on climate tipping elements exploiting the Coupled Model Intercomparison Project Phase 6 (CMIP6) archive, and particularly the outputs of the set of simulations performed under the AerChemMIP initiative. As such, all the results shown come from models where tropospheric chemistry and aerosols are explicitly simulated. The report first describes the analysis undertaken of the recent historical period (1950 to present), considering a set of experiments with identical forcings except for the emissions of NTCFs and their precursors (namely, *historical* and *hist-piNTCF*). Through this analysis, three main tipping elements have been selected: the Atlantic Meridional Overturning Circulation (AMOC), the Intertropical Convergence Zone and the Arctic, and the impact of NTCFs in their dynamics. Then, the analysis has focused on the assessment of the expected future evolution (2025-2054) of the AMOC and the North Atlantic circulation in scenarios with strong and weak air quality mitigation policies, but considerable levels of warming (namely, *ssp3370* and *ssp370-lowNTCF*). A weakening of the AMOC is detected in both future scenarios. Our analysis shows that more strict air quality policies would tend to accelerate this weakening.

CONTRIBUTION TO THE FOCI OBJECTIVES

The work described in this report contributes to the project objective O6:

"To undertake innovative and regionally relevant integrated analysis of optimised mitigation strategies, to support climate policy, deriving multiple benefits (e.g. climate mitigation and adaptation, human health, social, economic, and developmental), quantifying the sensitivity of climate system tipping points to non-CO2 forcers and meeting the global challenge of stabilising global temperatures and minimising the associated impacts on climate, weather, air quality and health"

1. INTRODUCTION

Climate tipping elements constitute components of the Earth System that are susceptible to undergo an abrupt, non-linear and potentially irreversible change in response to a perturbation (e.g., induced by warming). The critical threshold that triggers that non-linear response is usually termed “tipping-point”. Due to their high impact and potential consequences on a large fraction of the human population, the study of the effect of future warming on these tipping elements has gained attention in the last decades (Wunderling et al., 2023). However, the specific impact of Near-Term Climate Forcers (NTCFs) and their future evolution on tipping elements is yet understudied. The non-methane NTCFs, aerosols, tropospheric ozone and their precursors, are characterized by their relatively short atmospheric lifetimes and large spatio-temporal variability. Furthermore, aerosols, through their direct radiative effect, and semi-direct and indirect effect on clouds, have a net cooling effect on surface climate (Forster et al., 2021), opposed to the warming effect of greenhouse gases (GHGs), among which we can find NTCFs such as ozone or the well mixed and long lived species, e.g., CO2. Overall, increases in NTCFs during the historical period have partly masked the warming due to increases in GHGs. Given that in future scenarios the anthropogenic emissions of NTCFs are likely to be mitigated due to the implementation of stricter air quality policies, it is fundamental to understand their effect on climate tipping elements and their contribution to the triggering (or inhibition) of tipping points.

This deliverable presents the results of a multi-model analysis conducted relying on the Coupled Model Intercomparison Project Phase 6 (CMIP6, Eyring et al., 2016) ensemble, aimed at assessing potential impacts of NTCFs on climate tipping elements. In particular, this work quantifies the changes in the mean state and time evolution of well-known tipping elements in response to variations in NTCFs, with the aim of characterizing their potential to either weaken or strengthen the self-amplifying responses of these elements - signals that can serve as early warnings of approaching critical thresholds.

2. METHODOLOGY

We conducted a multi-model study using Earth System Model (ESM) data from the CMIP6. By considering multiple models, we aimed to increase the robustness and reliability of our results by reducing the influence of individual model biases and limitations (Tebaldi et al., 2007). For the purpose of this study, we require that the ESMs considered include comprehensive gas-phase chemistry schemes for simulating tropospheric ozone concentrations. Additionally, the models must simulate key aerosol species (both anthropogenic and natural) considering their interactions with clouds and radiation.

In particular, we used simulations from the CMIP6-AerChemMIP initiative, whose goal is to assess the impact of anthropogenic and natural atmospheric emissions, both in the past and under plausible future scenarios (Collins et al., 2017). We focused on those experiments that target the combined effects of anthropogenic non-methane NTCFs (aerosols, tropospheric ozone and their precursors). It must be noted that methane concentrations are prescribed in these simulations, and do not respond to NTCF emission changes. The time periods analysed are sufficiently long to detect climate responses (i.e., 30 years or more) and focus on the recent historical period (1950-2014) and the near future (2025-2054).

2.1 Historical period (1950-2014)

To assess the impacts of NTCF emissions on the recent past we compared two CMIP6 experiments: *historical* and *hist-piNTCF*. Both setups follow historical forcings, therefore capturing the climatic changes (both natural and anthropogenic) of the recent past. However, *hist-piNTCF* fixes anthropogenic, non-methane NTCF emissions at pre-industrial 1850 values.

In total, four models contributed to these experiments and fulfilled the requirement of having interactive chemistry and aerosols and publicly providing all the necessary variables for our analyses (see Table 1). All four models provide three members for each experiment, as this was the minimum requested by the AerChemMIP exercise, allowing us to better constrain the forced signals by averaging out some of the internal variability.

Table 1. List of models used in the historical study.

Model	Members	References
BCC-ESM1	r(1:3)i1p1f1	Wu et al. (2020)
EC-Earth3-AerChem	r(1,3,4)i1p1f1	van Noije et al. (2021)
MRI-ESM2-0	r(1,3,5)i1p1f1	Yukimoto et al. (2019), Deushi and Shibata (2011)
UKESM1-0-LL	r(1:3)i1p1f1	Sellar et al. (2019), Mulcahy et al. (2020)

We confined the study period to 1950-2014. Over this time frame atmospheric composition varied significantly. Global aerosol concentrations increased in the early decades, followed by stabilization from the 1980s onward, with regional differences in anthropogenic emissions. While Europe and North America implemented aerosol reduction measures, Asian emissions continued to rise (Tørseth et al., 2012; Klimont et al., 2017; Aas et al., 2019). It must be noted that recent studies indicate that the CMIP6 Community Emissions Data System (CEDS) dataset underestimates China's reductions in anthropogenic aerosol emissions during 2006-2014 (Wang et al., 2021). This potential bias should be considered when interpreting our results. In contrast, GHG concentrations, including tropospheric ozone, showed a continuous increase throughout the study period (Bauer et al., 2020; Griffiths et al., 2021). These divergent trends are particularly relevant, as most aerosol species and GHGs exert opposing net radiative effects at the top of the atmosphere (TOA), making their combined influence on climate a key aspect of our analysis.

2.2 Future Period (2025-2054)

To determine how different emission pathways of NTCFs can impact climate in the near future we considered two different CMIP6 experiments: *ssp370* and *ssp370-lowNTCF*. Both experiments are based on the Shared Socio-economic Pathway (SSP; Riahi et al., 2017) SSP3-7.0. This baseline scenario considers very unfavourable conditions, with societies facing high challenges both to mitigation and adaptation, and depicts a future with high emissions of NTCFs and high levels of warming (Fujimori et al., 2017).

Rao et al. (2017) delves into air pollution within the SSP scenarios and defines three narratives (strong, medium and weak pollution control) based on the ambition and effectiveness of air pollution policies. In this context, the difference between the experiments studied is that in *ssp370*, all air pollutants follow a weak pollution control pathway (SSP3), whereas in *ssp370-lowNTCF*, NTCF emissions follow a strong pollution control narrative (SSP1).

Table 2. List of models used in the projection study.

Model	Members	References
BCC-ESM1	r(1:3)i1p1f1	Wu et al. (2020)
CESM2-WACCM	*ssp370*: r(1:3)i1p1f1 *ssp370-lowNTCF*: r(1:3)i1p2f1	Danabasoglu et al. (2020), Gettelman et al. (2019)
EC-Earth3-AerChem	r(1,3,4)i1p1f1	van Noije et al. (2021)
GISS-E2-1-G	r(1:3)i1p3f1	Bauer et al. (2020), Nazarenko et al. (2022), Kelley et al. (2020)
MPI-ESM-1-2-HAM	r(1:3)i1p1f1	Mauritsen et al. (2019), Tegen et al. (2019), Neubauer et al. (2019)
MRI-ESM2-0	r(1,3,5)i1p1f1	Yukimoto et al. (2019), Deushi and Shibata (2011)
NorESM2-LM	r(1:3)i1p1f1	Seland et al. (2020), Kirkevåg et al. (2018)

Out of all the models that contributed to the CMIP6-AerChemMIP initiative for these two experiments, we selected those with interactive tropospheric chemistry and aerosols as well as AMOC variables available (i.e., *msftmz*, *msftyz* or *vmo*) for optimal interpretation of the Atlantic circulation. All seven models that were considered provide three members for both scenarios, resulting in a 21-member ensemble (see Table 2).

2.3 Statistical Analysis

For the formal analysis we focused on two main aspects: climatological mean differences and time series of differences in annual values. This approach allowed us to detect differences in the climate mean state attributable to NTCFs, as well as the temporal evolution of the signals.

To assess statistical significance, for climatological analyses we used paired-samples t-tests while for annual data we employed two-sample bootstrap tests with 5000 resamples (Efron, 1979; Mudelsee and Alkio, 2007), both at the 95% significance level.

3. RESULTS: HISTORICAL PERIOD (1950-2014)

We isolated the NTCFs signal by comparing the climatological mean of the *historical* and *hist-piNTCF* ensembles for key climate variables such as surface air temperature (*tas*) and precipitation (*pr*). This approach revealed three primary climate impacts: a global cooling effect, particularly pronounced in the Arctic; a substantial increase in Labrador Sea convection; and a southward displacement of tropical precipitation consistent with a shift of the Intertropical Convergence Zone (ITCZ). Each of these responses will be examined in detail in the following subsections.

3.1 NTCFs Impact on Arctic Temperature

Historical NTCFs drive a global cooling with the most intense signal located at Arctic latitudes (Fig. 1). We attribute this enhanced regional cooling to aerosols (Lewinschal et al., 2019; Westervelt et al., 2020), which counteract the warming effects of tropospheric ozone in this region (Sand et al., 2016).

Further analysis reveals that the Arctic cooling is most intense near the surface and during the boreal autumn and winter seasons, with temperature differences reaching down to -5°C. This temperature behaviour aligns with the Arctic Amplification (AA) phenomenon, in which the Arctic magnifies global temperature changes through the action of different regional positive feedbacks (Previdi et al., 2021).

To quantify the Arctic Amplification attributable to NTCFs, we computed the Arctic Amplification Factor (AAF; Eq. 1; Wu et al., 2024):

$$AAF = \frac{m(\Delta T_{arctic})}{m(\Delta T_{global})} \quad (1)$$

where ΔT_i represents the temperature difference between the *historical* and *hist-piNTCF* ensembles in the different regions (Fig. 2a,b), and m represents the slope of these signals (linear trends). For the period 1950–1980, the AAF of NTCFs is 3.87 for the multi-model mean, indicating that Arctic cooling due to NTCFs was nearly four times stronger than the global average. After the 1980s, however, this forcing diminishes in significance, and greenhouse gas (GHG) driven warming becomes the primary driver of both Arctic and global temperature trends.

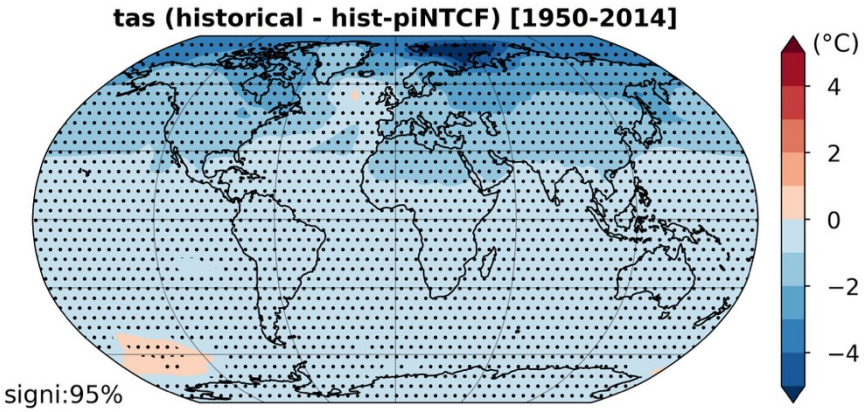

Figure 1. Surface air temperature (*tas*) response to historical NTCFs (1950-2014). Map shows the difference in *tas* climatologies between *historical* and *hist-piNTCF* experiments from a 4-model CMIP6 ensemble (BCC-ESM1, MRI-ESM2-0, UKESM1-0-LL, EC-Earth3-AerChem; 3 members each). Stippling indicates statistical significance at 95% confidence level (paired t-test).

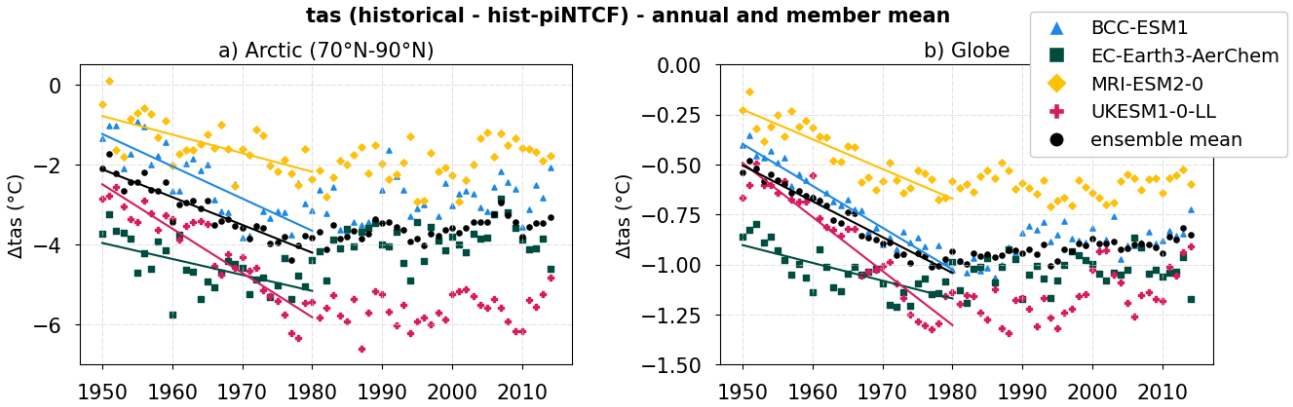

Figure 2. Annual surface air temperature (*tas*) response to historical NTCFs (1950-2014) for the (a) Arctic (70°N–90°N) and (b) global domains. Symbols show the difference between *historical* and *hist-piNTCF* CMIP6 experiments from a 4-model CMIP6 ensemble (BCC-ESM1 blue triangles, EC-Earth3-AerChem green squares,

MRI-ESM2-0 yellow diamonds and UKESM1-0-LL pink crosses); black circles show the multi-model mean. Solid lines indicate linear trends for 1950-1980. For each experiment and model we consider the mean of 3 members.

Our results suggest a consistent increase in sea ice extent with higher NTCF concentration, reinforcing the hypothesis of the amplified Arctic cooling being mediated by regional feedbacks (e.g., sea ice-albedo feedback). However, additional factors, such as variations in atmospheric (Needham and Randall, 2023) and oceanic (Iwi et al., 2012; Robson et al., 2022) energy transport, may also contribute to the observed temperature changes.

3.2 NTCFs Impact on Labrador Sea Convection

Historical NTCF concentrations drive an increase of the mixed layer depth (*mlotst*), a widely used proxy for oceanic convection, across various regions of the subpolar North Atlantic (Fig. 3a). Notably, we discarded two of the EC-Earth3-AerChem historical members for this analysis as they show signs of collapsed convection in the Labrador Sea. This is a well-documented issue of the model arising from spurious triggering of internal variability (Bilbao et al., 2021; Meccia et al., 2023).

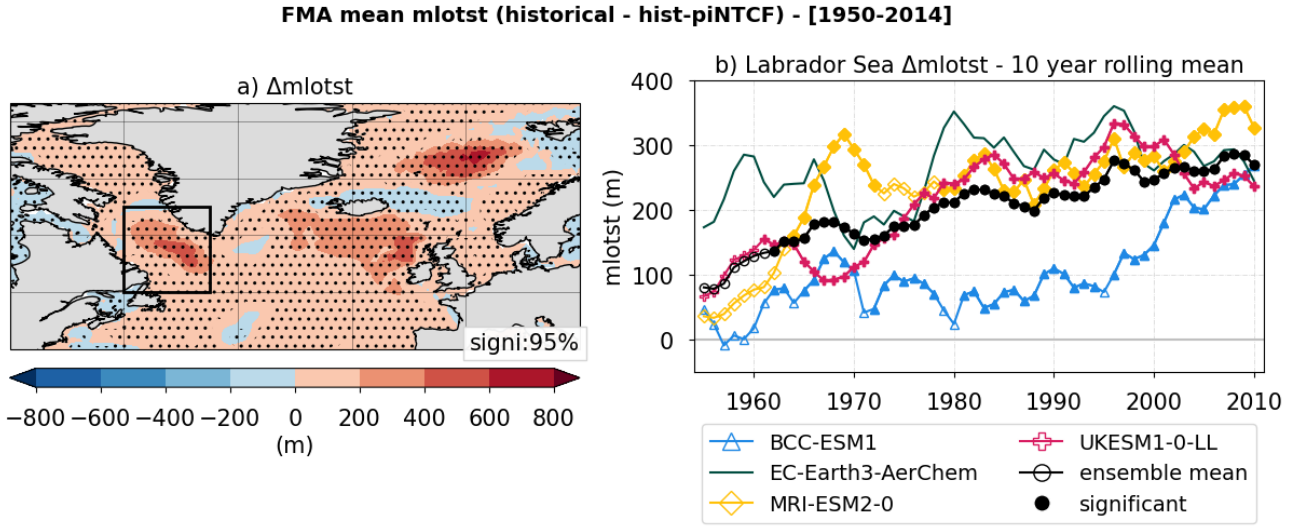

Figure 3. Ocean mixed layer thickness (*mlotst*) response to historical NTCFs during the maximum convection season (February-April, 1950-2014). Signal derived from the difference between *historical* and *hist-piNTCF* CMIP6 experiments using a 4-model ensemble (BCC-ESM1, MRI-ESM2-0, UKESM1-0-LL, EC-Earth3-AerChem). (a) *mlotst* climatology signal, significant where stippling is applied (95% confidence, paired t-test). The black box delineates the Labrador Sea region (60°W–45°W, 50°N–65°N). (b) Ten-year rolling mean of the Labrador Sea *mlotst* signal for the multi-model mean (black circles) and individual models (BCC-ESM1 blue triangles, EC-Earth3-AerChem green line, MRI-ESM2-0 yellow diamonds, UKESM1-0-LL pink crosses). Filled symbols indicate statistical significance (95% confidence, bootstrap test). Data represent 3-member ensemble means except EC-Earth3-AerChem (1 member; no significance testing in panel b).

To understand the mechanisms driving this convection increase, we focused on the Labrador Sea area (60°W–45°W; 50°N–65°N) as a region of agreement across all models in the ensemble. The temporal evolution of the mean convection signal in the Labrador Sea (Fig. 3b) shows a persistent enhancement of convection with

decadal oscillations that are not in phase across models. In particular, the multi-model mean indicates a 38% increase in Labrador Sea convection due to NTCFs from 1950 to 2014.

Further analysis of the water properties in the vertical column revealed colder and saltier sea surface conditions due to the effect of NTCFs. Both properties contribute to denser surface waters, thereby eroding stratification and promoting convection. While the temperature decrease aligns with the negative radiative forcing of aerosols discussed in the previous section, the surface salinity increase likely results from a positive feedback mechanism: stronger convection, initially driven by surface cooling, brings saltier subsurface waters to the surface, further increasing surface density and reinforcing deep convection. This feedback mechanism could explain the steady increase in mixed layer depth observed in Figure 3b, despite aerosol reductions after the 1980s.

Our findings suggest that aerosols are the main drivers of the convection signal, as evidenced by the surface cooling over the Labrador Sea. However, the precise mechanisms—whether through direct local forcing or via remote advection of aerosol-induced anomalies—remain to be fully determined (e.g., Menary et al., 2020; Hassan et al., 2021; Liu et al., 2024).

3.3 NTCFs Impact on Tropical Precipitation

Historical NTCFs induce a decrease in precipitation north of the equator and an increase to the south (Fig. 4a). This pattern is consistent with a southward displacement of the ITCZ, a phenomenon observed in response to aerosol increases in previous studies (Allen et al., 2015; Pausata et al., 2020; Zhao and Suzuki, 2021).

To quantify the ITCZ latitude changes, we first calculated the zonal mean precipitation from 20°S to 20°N. We then determined the coordinates of the precipitation centroid (PCENT), defined as the point that delineates regions of equal weight in the precipitation distribution. By comparing PCENT coordinates between the *historical* and *hist-piNTCF* ensembles, we quantified the effects of historical NTCFs on both ITCZ latitude (*Δlat*; Eq. 2) and precipitation amount (*Δpr*; Eq. 3):

$$\Delta lat = lat\left(PCENT_{historical}\right) - lat\left(PCENT_{hist-piNTCF}\right) \quad (2)$$

$$\Delta pr = pr\left(PCENT_{historical}\right) - pr\left(PCENT_{hist-piNTCF}\right) \quad (3)$$

The latitudinal ITCZ response for the multi-model mean reveals a mean southward displacement of 0.6° (Fig. 4b). For individual models, the signal exhibits multi-decadal oscillations, particularly prominent in MRI-ESM2-0 and BCC-ESM1. However, no evidence of a robust long-term trend emerges. In an analogous analysis of the precipitation amount change (Δpr), the multi-model ensemble mean shows an 2.0% ITCZ weakening due to historical NTCFs over 1950–2014 (not shown).

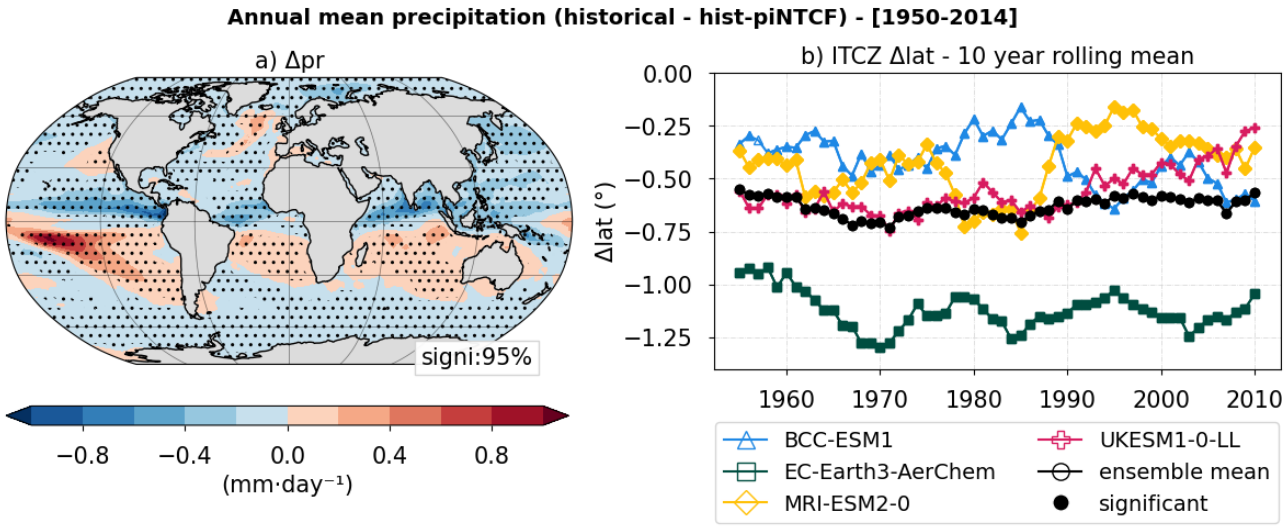

Figure 4. Precipitation response to historical NTCFs (1950-2014), derived from the difference between *historical* and *hist-piNTCF* CMIP6 experiments using a 4-model ensemble (BCC-ESM1, MRI-ESM2-0, UKESM1-0-LL, EC-Earth3-AerChem; 3 members each). (a) Climatological precipitation signal, significant where stippling is applied (95% confidence, paired t-test). (b) Ten-year rolling mean of ITCZ latitude shift for the multi-model mean (black circles) and the individual models (BCC-ESM1 blue triangles, EC-Earth3-AerChem green line, MRI-ESM2-0 yellow diamonds, UKESM1-0-LL pink crosses). Filled symbols indicate statistical significance (95% confidence, bootstrap test). The ITCZ latitude index calculated from the zonal precipitation centroid between 20°S–20°N.

We relate the ITCZ latitude shift to an interhemispheric energy imbalance. In our experiments, higher aerosol concentrations in the Northern Hemisphere align with decreased radiative energy in the NH and a southward displacement of the ITCZ, which could be partially compensating for the interhemispheric heat imbalance.

Our analysis revealed a consistent circulation shift in response to NTCFs. Although the underlying physical mechanisms warrant further investigation, we hypothesize a relevant role of aerosol-cloud interactions in mediating the radiative forcing, as revealed by an inverse relationship between the net radiation and the cloud cover (*clt*) signals in mid- to high latitudes (not shown; Andersen et al., 2023).

4. RESULTS: FUTURE PERIOD (2025-2054)

As shown in section 3.2, anthropogenic NTCFs resulted in increased convection in the subpolar North Atlantic during the historical period. Given the close connection between convection in this region and the AMOC, as well as its great relevance for future climate stability, we conducted an analogous multi-model study to isolate how future air quality policies targeting NTCFs may affect Atlantic Ocean circulation. By comparing the *ssp370* and *ssp370-lowNTCF* experiments, we assess the specific contribution of NTCF emissions to future circulation changes.

Our analysis revealed a general AMOC weakening under stricter NTCF emission policies, amplifying the greenhouse gas-driven AMOC decline. The response exhibited substantial inter-model differences, with no model reaching a tipping point within the study period. A deeper investigation into the subpolar gyre current

system revealed differing circulation responses among models, with potential impacts on Atlantic-Arctic water exchanges.

4.1 NTCFs Impact on AMOC strength

Higher NTCF emissions cause an intensification of Atlantic circulation as shown by the overturning mass streamfunction response (*msftmyz*; Fig. 5a). We quantified the AMOC response by measuring its strength as the mean *msftmyz* between 35°N–45°N at 500–1500 m depth. The time evolution of the signal shows a broad range in the intensity of responses across the models of the ensemble (Fig. 5b). Notably, the individual models exhibit strong decadal variability that is not in phase across them. For the ensemble mean, we quantify an AMOC increase of 3% by the end of the study period (Fig. 5b).

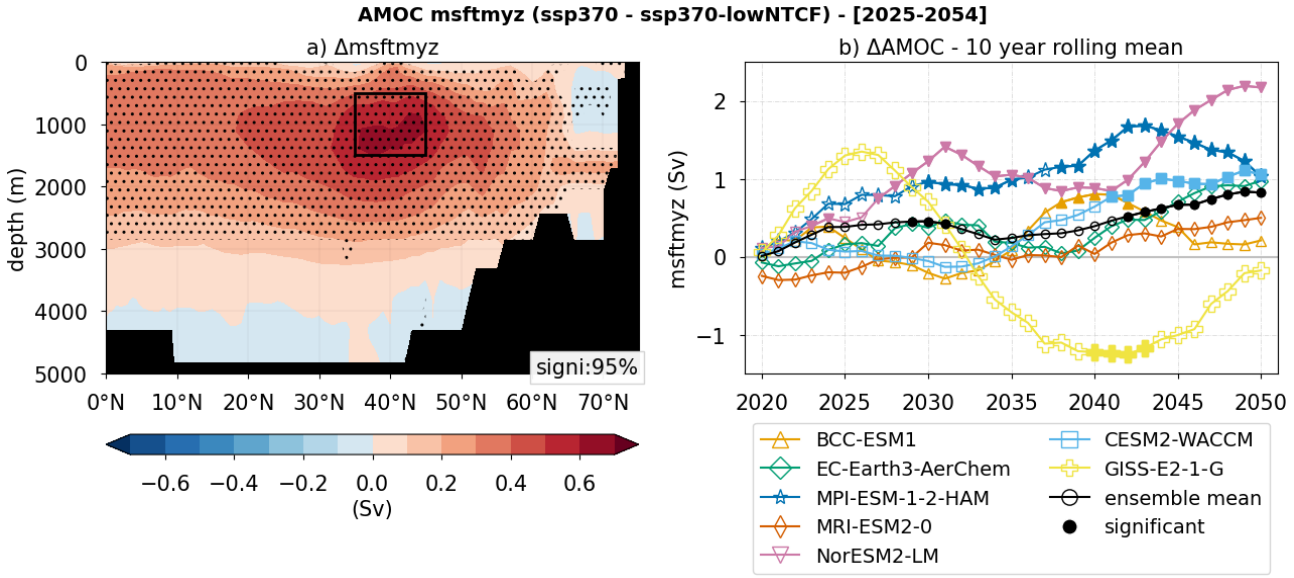

Figure 5. Future NTCF impacts on Atlantic meridional overturning circulation (2025-2054), derived from the difference between *ssp370* and *ssp370-lowNTCF* scenarios using a 7-model ensemble (BCC-ESM1, CESM2-WACCM, EC-Earth3-AerChem, GISS-E2-1-G, MPI-ESM-1-2-HAM, MRI-ESM2-0, NorESM2-LM; 3 members each). (a) Climatological difference in overturning mass streamfunction (*msftmyz*), significant where stippling is applied (95% confidence, paired t-test). (b) Ten-year rolling mean of AMOC strength differences for the multi-model mean (black circles) and the individual models (BCC-ESM1 orange triangles, CESM2-WACCM blue squares, EC-Earth3-AerChem green diamonds, GISS-E2-1-G yellow crosses, MPI-ESM-1-2-HAM blue stars, MRI-ESM2-0 red diamonds, NorESM2-LM pink inverted triangles). Filled symbols indicate statistical significance (95% confidence, bootstrap test). The AMOC index is defined as the mean *msftmyz* from 35°S–45°N, 500–1500m depth.

These results align with Hassan et al. (2022), who conducted a similar study with a four-model ensemble, also detecting an AMOC weakening in response to non-methane NTCF reductions, with substantial inter-model variability. They highlighted the outlier behaviour of the model GISS-E2-1-G, attributing it to the model being more sensitive to radiative forcing. Using the same scenarios, they reported that the AMOC response to NTCFs persists until the end of the century.

4.2 NTCFs Impact on the Subpolar Gyre

To understand the mechanisms driving the AMOC response to NTCFs, we examined changes in the Subpolar North Atlantic circulation system. As observed in the historical period (Fig. 3a), the future *mlotst* signal shows increased convection in the Labrador Sea area for the ensemble mean. GISS-E2-1-G remains an outlier, being the only model in which convection decreases in response to higher NTCF concentrations (not shown).

The response to future NTCFs is weaker than that detected in the historical study period, which is consistent with the smaller forcing difference between the two scenarios compared to the historical NTCF forcing relative to pre-industrial conditions.

Although we observed no common pattern across models, all of them show significant signals in at least one of three key regions: Labrador Sea (60°W–45°W, 50°N–66°N), Irminger Sea (45°W–25°W, 50°N–66°N), or Rockail Area (25°W–7°W, 50°N–63°N) (black boxes in Fig. 6).

Examining the vertical profiles of these regions, we observe that NTCFs produce an overall cooling in the Labrador and Irminger seas, which aligns with the detected increased water density. However, we find different salinity responses across models suggesting more complex mechanisms at play which warrant further investigation. In the Rockail area we also see a cooling, in this case accompanied by a salinification most intense at the surface, which results in an increased water density. We note that, in this region, MPI-ESM-1-2-HAM is an outlier, showing a surface warming along with the salinification (not shown).

The barotropic streamfunction (*msftbarot*) shows a broad range of responses to NTCFs across models (Fig. 6). While NorESM2-LM shows an overall strengthening of the gyre, CESM2-WACCM and MPI-ESM-1-2-HAM suggest a shift in gyre circulation with Labrador Sea intensification while showing a decrease in the Irminger Sea. GISS-E2-1-G shows a weakening of the Labrador Sea circulation, once again opposing the rest of the ensemble.

Regarding the Rockail Area, CESM2-WACCM and MPI-ESM-1-2-HAM exhibit decreased gyre circulation in the region along with increased cyclonic circulation in the Norwegian Sea. These two systems are connected by outflows and inflows that surround Iceland. Changes in these currents could potentially explain the *msftbarot* signals, though further investigation is ongoing.

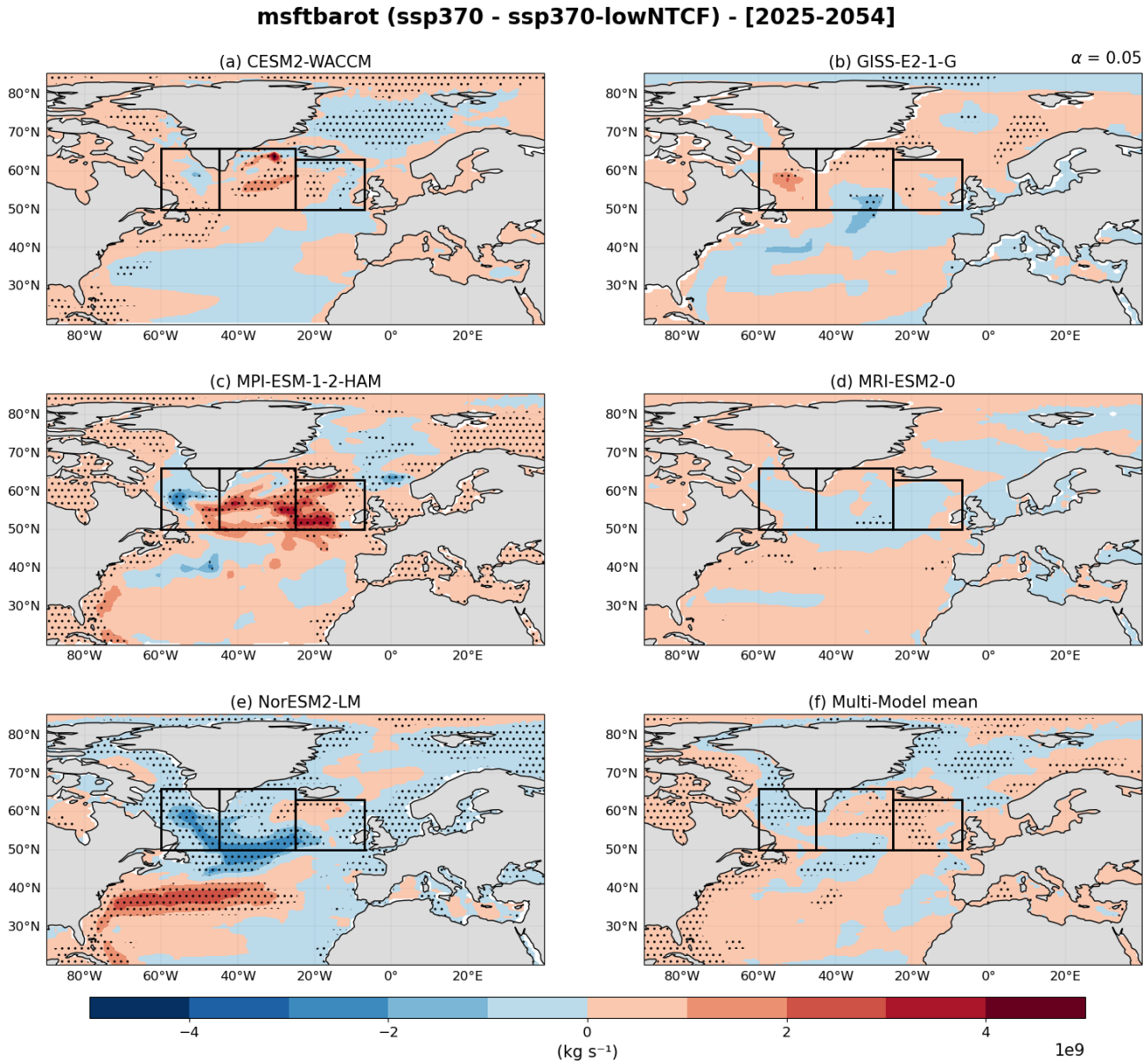

Figure 6. Barotropic mass streamfunction (*msftbarot*) response to future NTCFs (2025–2054). Map shows the difference in *msftbarot* climatologies between the *ssp370* and *ssp370-lowNTCF* scenarios for individual CMIP6 models: (a) MRI-ESM2-0, (b) MPI-ESM-1-2-HAM, (c) CESM2-WACCM, (d) NorESM2-LM, (e) GISS-E2-1-G, and (f) the multi-model mean. For each experiment and model we consider the mean of 3 members. Stippling indicates statistical significance at 95% confidence level (paired t-test). The black boxes denote key regions, from left to right: Labrador Sea (60°W–45°W, 50°N–65°N), Irminger Sea (45°W–25°W, 50°N–66°N) and Rockail Area (25°W–7°W, 50°N–63°N).

5. OUTLOOK

This study shows that the negative radiative forcing of aerosols dominates the historical NTCF impact on climate, counteracting the warming effects of absorbing aerosols and tropospheric ozone. During the recent historical period, multi-model mean analyses reveal three key climate responses: (1) a global cooling, amplified in the Arctic, where autumn temperatures decrease by up to 5°C; (2) a 38% increase in Labrador Sea ocean convection; and (3) changes in tropical precipitation, including a 0.6° southward displacement of the ITCZ and a 2.0% weakening of ITCZ intensity. In the future, NTCFs will continue to exert their influence on climate tipping elements. In particular, our analyses show a general AMOC weakening under stricter NTCF emission policies, amplifying the greenhouse gas-driven AMOC decline. The response signal exhibits substantial inter-model differences, with no model reaching a tipping point within the study period. A deeper investigation into the subpolar gyre current system revealed differing circulation responses between models, with potential impacts on Atlantic-Arctic water exchanges.

PUBLICATIONS

Santos-Espeso, A., Gonçalves Ageitos, M., Ortega, P., Pérez García-Pando, C., Donat, M. G., Samso Cabré, M., and Loosveldt Tomas, S.: Regional climate imprints of recent historical changes in anthropogenic Near Term Climate Forcers, EGUsphere [preprint], https://doi.org/10.5194/egusphere-2025-1286, 2025.

REFERENCES

Aas, W., Mortier, A., Bowersox, V., Cherian, R., et al.: Global and regional trends of atmospheric sulfur, Scientific Reports, 9, 953, https://doi.org/10.1038/s41598-018-37304-0, 2019.

Allen, R. J., Evan, A. T., Booth, B. B. B.: Interhemispheric aerosol radiative forcing and tropical precipitation shifts during the late twentieth century, Journal of Climate, 28, 8219–8246, doi:10.1175/JCLI-D-15-0148.1, 2015.

Andersen, H., Cermak, J., Douglas, A., Myers, T. A., Nowack, P., Stier, P., Wall, C. J., and Wilson Kemsley, S.: Sensitivities of cloud radiative effects to large-scale meteorology and aerosols from global observations, Atmospheric Chemistry and Physics, 23, 10 775–10 794, https://doi.org/10.5194/acp-23-10775-2023, 2023.

Bauer, S. E., Tsigaridis, K., Faluvegi, G., Kelley, M., Lo, K. K., Miller, R. L., Nazarenko, L., Schmidt, G. A., and Wu, J.: Historical (1850–2014) Aerosol Evolution and Role on Climate Forcing Using the GISS ModelE2.1 Contribution to CMIP6, Journal of Advances in Modeling Earth Systems, 12, e2019MS001 978, https://doi.org/10.1029/2019MS001978, 2020.

Bilbao, R., Wild, S., Ortega, P., Acosta-Navarro, J., et al.: Assessment of a full-field initialized decadal climate prediction system with the CMIP6 version of EC-Earth, Earth System Dynamics, 12, 173–196, https://doi.org/10.5194/esd-12-173-2021, 2021.

Collins, W. J., Lamarque, J.-F., Schulz, M., Boucher, O., et al.: AerChemMIP: quantifying the effects of chemistry and aerosols in CMIP6, Geoscientific Model Development, 10, 585–607, https://doi.org/10.5194/gmd-10-585-2017, 2017.

Danabasoglu, G., Lamarque, J.-F., Bacmeister, J., Bailey, D. A., DuVivier, A. K., Edwards, J., et al.: The Community Earth System Model Version 2 (CESM2), Journal of Advances in Modeling Earth Systems, 12, e2019MS001916, doi:10.1029/2019MS001916, 2020.

Deushi, M., Shibata, K.: Development of a Meteorological Research Institute Chemistry-Climate Model version 2 for the study of tropospheric and stratospheric chemistry, Papers in Meteorology and Geophysics, 62, 1–46, doi:10.2467/mripapers.62.1, 2011.

Efron, B.: Bootstrap Methods: Another Look at the Jackknife, The Annals of Statistics, 7, 1–26, https://doi.org/10.1214/aos/1176344552, 1979.

Eyring, V., Bony, S., Meehl, G. A., Senior, C. A., Stevens, B., Stouffer, R. J., and Taylor, K. E.: Overview of the Coupled Model Intercomparison Project Phase 6 (CMIP6) experimental design and organization, Geoscientific Model Development, 9, 1937–1958, https://doi.org/10.5194/gmd-9-1937-2016, 2016.

Forster, P., T. Storelvmo, K. Armour, W. Collins, et al.: The Earth's Energy Budget, Climate Feedbacks, and Climate Sensitivity. In Climate Change 2021: The Physical Science Basis. Contribution of Working Group I to the Sixth Assessment Report of the Intergovernmental Panel on Climate Change [Masson-Delmotte, V., et al.(eds.)]. Cambridge University Press, Cambridge, United Kingdom and New York, NY, USA, pp. 923–1054, doi:10.1017/9781009157896.009, 2021.

Fujimori, S., Hasegawa, T., Masui, T., Takahashi, K., Herran, D. S., Dai, H., Hijioka, Y., and Kainuma, M.: SSP3: AIM implementation of Shared Socioeconomic Pathways, Global Environmental Change, 42, 268–283, https://doi.org/10.1016/j.gloenvcha.2016.06.009, 2017.

Gettelman, A., Mills, M. J., Kinnison, D. E., Garcia, R. R., et al.: The whole atmosphere community climate model version 6 (WACCM6), Journal of Geophysical Research: Atmospheres, 124, 12380–12403, doi:10.1029/2019JD030943, 2019.

Griffiths, P. T., Murray, L. T., Zeng, G., Shin, Y. M., et al.: Tropospheric ozone in CMIP6 simulations, Atmospheric Chemistry and Physics, 21, 4187–4218, https://doi.org/10.5194/acp-21-4187-2021, 2021.

Hassan, T., Allen, R. J., Liu, W., and Randles, C. A.: Anthropogenic aerosol forcing of the Atlantic meridional overturning circulation and the associated mechanisms in CMIP6 models, Atmospheric Chemistry and Physics, 21, 5821–5846, https://doi.org/10.5194/acp-21-5821-2021, 2021.

Hassan, T., Allen, R. J., Liu, W., Shim, S., van Noije, T., Le Sager, P., Oshima, N., Deushi, M., Randles, C. A., and O'Connor, F. M.: Air quality improvements are projected to weaken the Atlantic meridional overturning circulation through radiative forcing effects, Communications Earth & Environment, 3, 1–12, https://doi.org/10.1038/s43247-022-00476-9, 2022.

Iwi, A. M., Hermanson, L., Haines, K., and Sutton, R. T.: Mechanisms Linking Volcanic Aerosols to the Atlantic Meridional Overturning Circulation, Journal of Climate, https://doi.org/10.1175/2011JCLI4067.1, 2012.

Kelley, M., Schmidt, G. A., Nazarenko, L., Bauer, S. E., et al.: GISS-E2.1: Configurations and climatology, Journal of Advances in Modeling Earth Systems, 12, e2019MS002025, doi:10.1029/2019MS002025, 2020.

Kirkevåg, A., Grini, A., Olivié, D., Seland, Ø., et al.: A production-tagged aerosol module for Earth system models, OsloAero5.3 – extensions and updates for CAM5.3-Oslo, Geoscientific Model Development, 11, 3945–3982, https://doi.org/10.5194/gmd-11-3945-2018, 2018.

Klimont, Z., Kupiainen, K., Heyes, C., Purohit, P., Cofala, J., Rafaj, P., Borken-Kleefeld, J., and Schöpp, W.: Global anthropogenic emissions of particulate matter including black carbon, Atmospheric Chemistry and Physics, 17, 8681–8723, https://doi.org/10.5194/acp-17-8681-2017, 2017.

Lewinschal, A., Ekman, A. M. L., Hansson, H.-C., Sand, M., Berntsen, T. K., and Langner, J.: Local and remote temperature response of regional SO2 emissions, Atmospheric Chemistry and Physics, 19, 2385–2403, https://doi.org/10.5194/acp-19-2385-2019, 2019.

Liu, F., Li, X., Luo, Y., Cai, W., Lu, J., Zheng, X. T., Kang, S. M., Wang, H., Zhou, L.: Increased Asian aerosols drive a slowdown of Atlantic Meridional Overturning Circulation, Nature Communications, 15, 18, doi:10.1038/s41467-023-44597-x, 2024.

Mauritsen, T., Bader, J., Becker, T., Behrens, J., et al.: Developments in the MPI-M Earth System Model version 1.2 (MPI-ESM1.2) and its response to increasing CO_2, Journal of Advances in Modeling Earth Systems, 11, 998–1038, doi:10.1029/2018MS001400, 2019.

Meccia, V. L., Fuentes-Franco, R., Davini, P., Bellomo, K., Fabiano, F., Yang, S., and von Hardenberg, J.: Internal multi-centennial variability of the Atlantic Meridional Overturning Circulation simulated by EC-Earth3, Climate Dynamics, 60, 3695–3712, https://doi.org/10.1007/s00382-022-06534-4, 2023.

Menary, M. B., Robson, J., Allan, R. P., Booth, B. B. B., et al.: Aerosol-forced AMOC changes in CMIP6 historical simulations, Geophysical Research Letters, 47, e2020GL088166, doi:10.1029/2020GL088166, 2020.

Mudelsee, M. and Alkio, M.: Quantifying effects in two-sample environmental experiments using bootstrap confidence intervals, Environmental Modelling & Software, 22, 84–96, https://doi.org/10.1016/j.envsoft.2005.12.001, 2007.

Mulcahy, J. P., Johnson, C., Jones, C. G., Povey, A. C., et al.: Description and evaluation of aerosol in UKESM1 and HadGEM3-GC3.1 CMIP6 historical simulations, Geoscientific Model Development, 13, 6383–6423, https://doi.org/10.5194/gmd-13-6383-2020, 2020.

Nazarenko, L. S., Tausnev, N., Russell, G. L., Rind, D., et al.: Future climate change under SSP emission scenarios with GISS-E2.1, Journal of Advances in Modeling Earth Systems, 14, e2021MS002871, doi:10.1029/2021MS002871, 2022.

Neubauer, D., Ferrachat, S., Siegenthaler-Le Drian, C., Stier, P., Partridge, D. G., Tegen, I., Bey, I., Stanelle, T., Kokkola, H., and Lohmann, U.: The global aerosol–climate model ECHAM6.3–HAM2.3 – Part 2: Cloud evaluation, aerosol radiative forcing, and climate sensitivity, Geoscientific Model Development, 12, 3609–3639, https://doi.org/10.5194/gmd-12-3609-2019, 2019.

Needham, M. R. and Randall, D. A.: Anomalous Northward Energy Transport due to Anthropogenic Aerosols during the Twentieth Century, Journal of Climate, https://doi.org/10.1175/JCLI-D-22-0798.1, 2023.

Pausata, F. S. R., Zanchettin, D., Karamperidou, C., Caballero, R., and Battisti, D. S.: ITCZ shift and extratropical teleconnections drive ENSO response to volcanic eruptions, Science Advances, 6, eaaz5006, https://doi.org/10.1126/sciadv.aaz5006, 2020.

Previdi, M., Smith, K. L., and Polvani, L. M.: Arctic amplification of climate change: a review of underlying mechanisms, Environmental Research Letters, 16, 093 003, https://doi.org/10.1088/1748-9326/ac1c29, 2021.

Rao, S., Klimont, Z., Smith, S. J., Van Dingenen, et al.: Future air pollution in the Shared Socio-economic Pathways, Global Environmental Change, 42, 346–358, https://doi.org/10.1016/j.gloenvcha.2016.05.012, 2017.

Riahi, K., van Vuuren, D. P., Kriegler, E., Edmonds, J. et al.: The Shared Socioeconomic Pathways and their energy, land use, and greenhouse gas emissions implications: An overview, Global Environmental Change, 42, 153–168, https://doi.org/10.1016/j.gloenvcha.2016.05.009, 2017.

Robson, J., Menary, M. B., Sutton, R. T., Mecking, J., et al.: The Role of Anthropogenic Aerosol Forcing in the 1850–1985 Strengthening of the AMOC in CMIP6 Historical Simulations, Journal of Climate, 35, 6843–6863, https://doi.org/10.1175/JCLI-D-22-0124.1, 2022.

Sand, M., Berntsen, T. K., von Salzen, K., Flanner, M. G., Langner, J., and Victor, D. G.: Response of Arctic temperature to changes in emissions of short-lived climate forcers, Nature Climate Change, 6, 286–289, https://doi.org/10.1038/nclimate2880, 2016.

Seland, Ø., Bentsen, M., Olivié, D., Toniazzo, T., et al.: Overview of the Norwegian Earth System Model (NorESM2) and key climate response of CMIP6 DECK, historical, and scenario simulations, Geoscientific Model Development, 13, 6165–6200, https://doi.org/10.5194/gmd-13-6165-2020, 2020.

Sellar, A. A., Jones, C. G., Mulcahy, J. P., Tang, Y., et al.: UKESM1: Description and Evaluation of the U.K. Earth System Model, Journal of Advances in Modeling Earth Systems, 11, 4513–4558, https://doi.org/10.1029/2019MS001739, 2019.

Tebaldi, C. and Knutti, R.: The use of the multi-model ensemble in probabilistic climate projections, Philosophical Transactions of the Royal Society A: Mathematical, Physical and Engineering Sciences, 365, 2053–2075, https://doi.org/10.1098/rsta.2007.2076, 2007.

Tegen, I., Neubauer, D., Ferrachat, S., Siegenthaler-Le Drian, C., et al.: The global aerosol–climate model ECHAM6.3–HAM2.3 – Part 1: Aerosol evaluation, Geoscientific Model Development, 12, 1643–1677, https://doi.org/10.5194/gmd-12-1643-2019, 2019.

Tørseth, K., Aas, W., Breivik, K., Fjæraa, A. M., Fiebig, M., Hjellbrekke, A. G., Lund Myhre, C., Solberg, S., and Yttri, K. E.: Introduction to the European Monitoring and Evaluation Programme (EMEP) and observed atmospheric composition change during 1972–2009, Atmospheric Chemistry and Physics, 12, 5447–5481, https://doi.org/10.5194/acp-12-5447-2012, 2012.

van Noije, T., Bergman, T., Le Sager, P., O'Donnell, D., et al.: EC-Earth3-AerChem: a global climate model with interactive aerosols and atmospheric chemistry participating in CMIP6 , Geosci. Model Dev., 14, 5637–5668, https://doi.org/10.5194/gmd-14-5637-2021, 2021.

Wang, Z., Lin, L., Xu, Y., Che, H., Zhang, X., Zhang, H., Dong, W., Wang, C., Gui, K., and Xie, B.: Incorrect Asian aerosols affecting the attribution and projection of regional climate change in CMIP6 models, npj Climate and Atmospheric Science, 4, 1–8, https://doi.org/10.1038/s41612-020-00159-2, 2021.

Westervelt, D. M., Mascioli, N. R., Fiore, A. M., Conley, A. J., Lamarque, J.-F., Shindell, D. T., Faluvegi, G., Previdi, M., Correa, G., and Horowitz, L. W.: Local and remote mean and extreme temperature response to regional aerosol emissions reductions, Atmospheric Chemistry and Physics, 20, 3009–3027, https://doi.org/10.5194/acp-20-3009-2020, 2020.

Wunderling, N., von der Heydt, A. S., Aksenov, Y., Barker, S., et al.: Climate tipping point interactions and cascades: a review, Earth System Dynamics, 15, 41–74, https://doi.org/10.5194/esd-15-41-2024, 2024.

Wu, T., Zhang, F., Zhang, J., Jie, W.,et al.: Beijing Climate Center Earth System Model version 1 (BCC-ESM1): model description and evaluation of aerosol simulations, Geoscientific Model Development, 13, 977–1005, https://doi.org/10.5194/gmd-13-977-2020, 2020.

Wu, Y.-T., Liang, Y.-C., Previdi, M., Polvani, L. M., England, M. R., Sigmond, M., and Lo, M.-H.: Stronger Arctic amplification from anthropogenic aerosols than from greenhouse gases, npj Climate and Atmospheric Science, 7, 1–7, https://doi.org/10.1038/s41612-024-00696-0, 2024.

Yukimoto, S., Kawai, H., Koshiro, T., Oshima, N., et al.: The Meteorological Research Institute Earth System Model Version 2.0, MRI-ESM2.0: Description and Basic Evaluation of the Physical Component, Journal of the Meteorological Society of Japan. Ser. II, 97, 931–965, https://doi.org/10.2151/jmsj.2019-051, 2019.

Zhao, S. and Suzuki, K.: Exploring the Impacts of Aerosols on ITCZ Position Through Altering Different Autoconversion Schemes and Cumulus Parameterizations, Journal of Geophysical Research: Atmospheres, 126, e2021JD034 803, https://doi.org/10.1029/2021JD034803, 2021.